Drift reduction in IMU-only pedestrian navigation system in unstructured environment

Conference Paper · May 2015

DOI: 10.1109/ASCC.2015.7244849

4 authors, including:

Muhammad Ilyas
University of Science and Technology, Korea

Kuk Cho
Korea Institute of Industrial Technology

Sangdeok Park
Korea Institute of Industrial Technonogy

Drift Reduction in IMU-Only Pedestrian Navigation System in Unstructured Environment

Muhammad Ilyas
Intelligent Robot Engineering
University of Science and Technology (UST)
Daejon, South Korea
snulove@yahoo.com

Kuk Cho, Seung-Ho Baeg* and Sangdeok Park
Robotics R&BD Group
Korea Institute of Industrial Technology (KITECH)
Ansan-si , South Korea
{googi33, shbaeg, sdpark@kitech.re.kr}

***Abstract*—This paper aims at developing algorithmic approach to reduce the error drift in navigation information using only single motion sensor i.e. inertial measurement unit (IMU) in an unstructured environment. The target application is pedestrian navigation system (PNS), but these algorithms are general for other applications too involving autonomous systems. A MEMS IMU is mounted on the foot of the agent in order to get benefit of known walking patterns of the wearer. Algorithms are derived based on motion constraints of human walking and applied to reduce the inherent error drift in inertial navigation systems (INS). Experiments are conducted in indoor/outdoor unstructured environment to validate this algorithmic approach and shown that without using any other sensors and any other pre-conditions on the environment; we can reduce navigation errors significantly only by taking into account the motion constraints of human walking.**

Keywords—pedestrian navigation system, inertial navigation, zero velocity update(ZUPT), data fusion.

I. INTRODUCTION

With the advent of miniaturized modern technology and powerful computing resources, the concept of the 'Ubiquitous Localization' is ready to fulfill soon. The core topic in ubiquitous localization is to track position of persons anywhere/any time i.e. indoor or outdoor with an accuracy of few meters. The Location based services (LBS) are being used and investigated using variety of sensor and systems e.g. using GPS signals, RFID, WLAN/WiFi, ultrasound, radio or vision technology [1] which requires, mostly, the pre-preparation of the environment to be used for localization. But in many cases to install the sensors in an environment pre-handed is impossible e.g. in hostile or hazardous environment, dangerous or collapsed buildings, emergency situations etc. Therefore, beacon-free solutions are preferably more appealing since they do not depend on any pre-installed infrastructure [2].

The infrastructure-free localization has been researched heavily during the last decades. Algorithms and systems have been proposed for accurate personal localization based on inertial sensors only [2], [14]. The inertial sensors are used in two ways within pedestrian navigation system. In first approach, called Pedestrian Dead-Reckoning (PDR) solutions, the constant step length of the wearer is assumed on a smooth surface, often usable in office environment. They integrate average step lengths and orientation estimates obtained from IMU at each detected step, so as to compute the absolute position and orientation of a person. This approach has the benefit of being simple and do not depend on the double integration of accelerometer signals to get position estimates, which are prone to large drifts unless corrected by some absolute knowledge. The downside of PDR is that they work on smooth surfaces and assume equal step length and need tuning for a specific user. The second approach, called inertial navigation system is adapted from aerospace research community, in which IMU is used at high rate for position, velocity and attitude (PVA) tracking of the platform on which it is strapped-down [3], [4]. This approach is fully independent of any kind of pre-condition of the user and the environment and is considered as an ideal approach in PVA tracking applications. But problem in INS is that the signals from IMU contain some kind of noise, and when these signals are integrated to get position by double integration of accelerometer signal, and attitude by single integration of gyro signals; the noise in the IMU signal also gets integrated which causes the error growth in PVA with the passage of time. To circumvent this problem, GPS is often used in outdoor navigation applications. However from pedestrian navigation perspective, human are not always under the open sky; hence GPS is not a reliable aiding source to INS. Using other sensors make the system more dependent, complex and costly/bulky; hence we investigate to use only single sensor (IMU) fitted on the foot of the wearer and assume no pre-condition on the user walking and the environment.

In this paper, we detect the waking patterns of the agent and apply appropriate algorithm to reduce the drift in INS solution. We concentrate on the following motion patterns:

- Stance phase i.e. foot fall on ground
- Walking in straight paths
- Standing still for long time

Further layout of this paper is as follows: In section II we describe the INS equations in details, Section III explains the INS aiding with virtual sensors (motion constraints); in section IV we present the experimental work and results; finally

*Corresponding author

978-1-4799-7862-5/15/$31.00 © 2015 IEEE

section V concludes this work with some future research foresights.

II. Foot-mounted Inertial Navigation System

A. Inertial navigation system (INS)

Inertial sensors have long been used on many underwater, land, air, space or even on other planets to navigate autonomous vehicles successfully [5]. But such applications often require high-grade IMUs, which are costly and bulky, to navigate reliably for extended periods of time, even though no aiding signal is available for INS.

In pedestrian navigation application, the main constraint is size and cost of the sensors used so that they can be fitted on human body with little extra effort. For that MEMS IMUs are preferred but they have drawback of having perturbed by large amount of noise in their signals which results in error drift in INS solution with time.

The advantages of INS lie in their ability to track motion of the agent at high rate without any external disturbance. An INS is a navigation system which depends entirely on inertial measurements. An IMU consists of three orthogonally aligned accelerometers which measure the linear acceleration and gravity acceleration and three gyroscopes which measure the angular rotation of the system on which they are mounted. Using these measurements from the IMU, the INS can calculate the current attitude, velocity and position of the platform given the initial PVA at starting time, called 'INS mechanization equations' presented in the next section.

B. Foot-mounted INS Mechanization

Inertial navigation system mechanization equations are a set of equations which form the basis of inertial navigation in a given navigation frame. Depending on the application, these equations take slightly different form in different navigation frames. It is well known that IMU output is related to the navigation information (i.e. PVA) through kinematic equations, known as 'INS Mechanization' [6]. The velocity of the agent in navigation frame is expressed as follows:

$$\dot{\mathbf{V}}^{\mathbf{n}} = \mathbf{C}_{\mathbf{b}}^{\mathbf{n}}\mathbf{f}^{\mathbf{b}} - \left(2\boldsymbol{\omega}_{\mathbf{ie}}^{\mathbf{n}} + \boldsymbol{\omega}_{\mathbf{en}}^{\mathbf{n}}\right)\times \mathbf{V}^{\mathbf{n}} + \mathbf{g}^{\mathbf{n}} \tag{1}$$

The first term on the R.H.S is the specific force (SF) experienced by accelerometer transformed in navigation frame by transformation matrix ($\mathbf{C}_{\mathbf{b}}^{\mathbf{n}}$), which in turn is formed by angular rates sensed by gyroscopic. The second term is the Coriolis acceleration due to the rotation of the Earth itself and last term is the effective gravity expressed in local navigation frame. The terms $\boldsymbol{\omega}_{\mathbf{ie}}^{\mathbf{n}}$ and $\boldsymbol{\omega}_{\mathbf{en}}^{\mathbf{n}}$, are the Earth rotation vector and navigation frame transport rate vector respectively, which are ignored for PNS. Hence the effective acceleration for PNS application in Earth fixed, locally tangent frame is expressed as:

$$\dot{\mathbf{V}}^{\mathbf{n}} = \mathbf{C}_{\mathbf{b}}^{\mathbf{n}}\mathbf{f}^{\mathbf{b}} + \mathbf{g}^{\mathbf{n}} \tag{2}$$

The equation (2) gives gravity compensated acceleration in n-frame. It is integrated numerically to get velocity and further integration will give position in n-frame (3, 4).

$$\mathbf{V}_{\mathbf{k}}^{\mathbf{n}} = \mathbf{V}_{\mathbf{k-1}}^{\mathbf{n}} + \int_{k-1}^{k} \dot{\mathbf{V}}^{\mathbf{n}}(\tau)d\tau \tag{3}$$

$$\mathbf{P}_{\mathbf{k}}^{\mathbf{n}} = \mathbf{P}_{\mathbf{k-1}}^{\mathbf{n}} + \int_{k-1}^{k} \mathbf{V}^{\mathbf{n}}(\tau)d\tau \tag{4}$$

The attitude update equations for foot-mounted PNS are derived from gyro inputs and are expressed in quaternion form in this work. Quaternion is a four-element vector representing rotation vector and magnitude of the rotation about that vector. The quaternion differential equation provides a relation between the input angular rates and the attitude quaternion, as shown in flowing equation:

$$\dot{\mathbf{q}} = \frac{1}{2}\mathbf{q}\otimes\tilde{\boldsymbol{\omega}}_{\mathbf{nb}}^{\mathbf{b}} \quad \therefore \tilde{\boldsymbol{\omega}}_{\mathbf{nb}}^{\mathbf{b}} \approx \boldsymbol{\omega}_{\mathbf{ib}}^{\mathbf{b}} \tag{5}$$

where $\tilde{\boldsymbol{\omega}}_{\mathbf{nb}}^{\mathbf{b}}$ is the quaternion form of the angular rates, which is function of gyro inputs, and product symbol ($\otimes$) represents the quaternion multiplication. If rotation vector is written in skew-symmetric form, (5) can be written in vector-matrix multiplication form as:

$$\dot{\mathbf{q}} = \frac{1}{2}[\tilde{\boldsymbol{\omega}}_{\mathbf{nb}}^{\mathbf{b}}\times]\mathbf{q} \quad \therefore [\tilde{\boldsymbol{\omega}}_{\mathbf{nb}}^{\mathbf{b}}\times] = \begin{bmatrix} 0 & -\omega_x & -\omega_y & -\omega_z \\ \omega_x & 0 & \omega_z & -\omega_y \\ \omega_y & -\omega_z & 0 & \omega_x \\ \omega_z & \omega_y & -\omega_x & 0 \end{bmatrix} \tag{6}$$

where the components of rotation vectors comes from gyro measurements. In discrete form, the (6) is written as:

$$\mathbf{q}_{\mathbf{k}} = [\boldsymbol{\Delta}\times]\mathbf{q}_{\mathbf{k-1}} \qquad \therefore \phi = \sqrt{\omega_x^2 + \omega_y^2 + \omega_z^2} \tag{7}$$

$$[\boldsymbol{\Delta}] = \begin{bmatrix} \cos(\phi/2) & \frac{1}{\phi}\sin(\phi/2)\phi_x & \frac{1}{\phi}\sin(\phi/2)\phi_y & \frac{1}{\phi}\sin(\phi/2)\phi_z \end{bmatrix}^T$$

where $[\Delta\times]$ is the skew-symmetric form of the vector $[\Delta]$. The updated quaternion components are used to form the transformation matrix from body (b) frame to n-frame, i.e.

$$\mathbf{C}_{\mathbf{b}}^{\mathbf{n}}(k) = \begin{bmatrix} q_0^2+q_1^2-q_2^2-q_3^2 & -2(q_0q_3-q_1q_2) & 2(q_0q_2+q_1q_3) \\ 2(q_0q_3+q_1q_2) & q_0^2-q_1^2+q_2^2-q_3^2 & -2(q_0q_1-q_2q_3) \\ -2(q_0q_2-q_1q_3) & 2(q_0q_1+q_2q_3) & q_0^2-q_1^2-q_2^2+q_3^2 \end{bmatrix} \tag{8}$$

This transformation matrix is used to transform the accelerometer sensed linear acceleration in b-frame to corresponding acceleration in n-frame, as in equation (2). The equations (3, 4 and 7) are used to propagate the PVA of the walker with only inputs from the foot-mounted IMU. In compact form, the INS mechanization equation is given in (9) below:

$$\begin{bmatrix} \mathbf{P}_k^n \\ \mathbf{v}_k^n \\ \mathbf{C}_{b,k}^n \end{bmatrix} = \begin{bmatrix} \mathbf{P}_{k-1}^n + \mathbf{v}_{k-1}^n\Delta T \\ \mathbf{v}_{k-1}^n + \left\{\mathbf{C}_b^n\mathbf{f}^b + \mathbf{g}^n\right\}\Delta T \\ \mathbf{C}_{b,k-1}^n + \Omega(\mathbf{q}, \boldsymbol{\omega}_{ib}^b, \Delta T) \end{bmatrix} + \begin{bmatrix} w^p \\ w^v \\ w^\psi \end{bmatrix} \tag{9}$$

$$\therefore \mathbf{X}_{\mathbf{k}} = \mathbf{f}(\mathbf{X}_{\mathbf{k-1}}, \mathbf{f}^b, \Delta T) + \mathbf{w}$$

where $\Omega(.)$ is a function of gyro measurements, updated during the sampling time interval ΔT . One update processing cycle of PVA in INS is shown in Fig. 1.

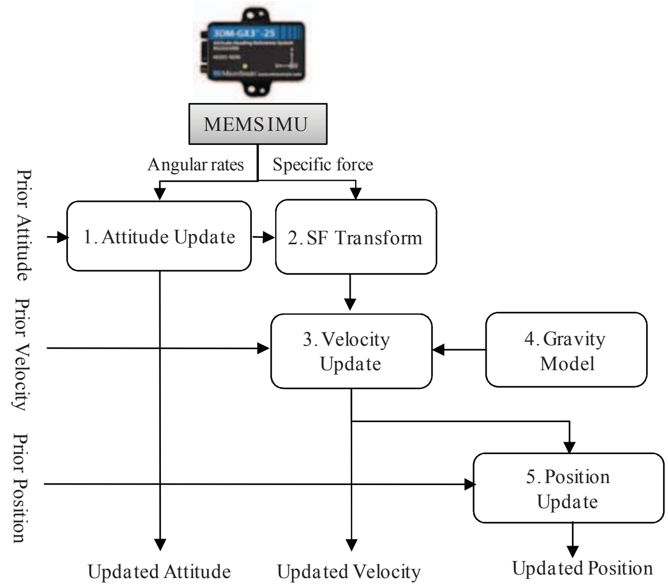

Fig. 1. Inertial navigation system (INS) computation steps [3].

C. Foot-mounted INS Error Model

In order to estimate the errors in INS produced PVA, one must derive the INS error model which can be used in Kalman filter estimator. Details of INS error model derivation are given in [3], [6]. In nutshell, the standard strapdown error navigation equations using phi-angle error model are given below:

$$\boldsymbol{\delta}\dot{\mathbf{v}}^n = \left[\boldsymbol{\delta\psi}^n \times\right]\mathbf{f}^n + \mathbf{C}_b^n\delta\mathbf{f}^b - 2(\boldsymbol{\delta\omega}_{in}^n \times \mathbf{v}^n + \boldsymbol{\omega}_{in}^n \times \boldsymbol{\delta}\mathbf{v}^n) + \boldsymbol{\delta}g^n \tag{10}$$

Since the navigation frame is fixed on the Earth, the error in the angular rate ($\boldsymbol{\delta\omega}_{in}^n$) of the navigation frame is zero. For simplification, the gravity error ($\boldsymbol{\delta}g^n$) is also assumed to be zero. For PNS application, the Coriolis acceleration caused by velocity error is also neglected here. Finally, after rearranging, (10) becomes;

$$\boldsymbol{\delta}\dot{\mathbf{v}}^n = \mathbf{C}_b^n[\mathbf{f}^b \times]\boldsymbol{\delta\psi}^n + \mathbf{C}_b^n\delta\mathbf{f}^b \tag{11}$$

where $[\mathbf{f}^b \times]$ Skew-symmetric form of acceleration is, $\boldsymbol{\delta\psi}^n$ is the misalignment error vector and $\delta\mathbf{f}^b$ are the accelerometer measurement error vector. Similarly, the position errors are modeled as:

$$\boldsymbol{\delta}\dot{\mathbf{P}}^n = \left[-\boldsymbol{\omega}_{en}^n \times \boldsymbol{\delta}\mathbf{P}^n\right] + \delta\boldsymbol{\theta} \times \mathbf{v}^n + \delta\mathbf{v}^n \tag{12}$$

Here, $\boldsymbol{\omega}_{en}^n$ is the transport rate of n-frame w.r.t Earth, which is ignored in PNS application, $\delta\boldsymbol{\theta}$ is the angle between true frame and n-frame, again a negligible term for PNS applications. Hence the position error model for foot-mounted IMU is:

$$\boldsymbol{\delta}\dot{\mathbf{P}}^n = \delta\mathbf{v}^n \tag{13}$$

Finally, the attitude error model in this representation is expressed as:

$$\boldsymbol{\delta}\dot{\boldsymbol{\psi}}^n = -\boldsymbol{\omega}_{in}^n \times \boldsymbol{\delta\psi}^n - \mathbf{C}_b^n\boldsymbol{\delta\omega}_{ib}^b + \boldsymbol{\delta\omega}_{in}^n \tag{14}$$

The first and third terms are zero for Earth fixed frame, so error model for attitude angles in n-frame for PNS application is:

$$\boldsymbol{\delta}\dot{\boldsymbol{\psi}}^n = -\mathbf{C}_b^n\boldsymbol{\delta\omega}_{ib}^b \tag{15}$$

The equation (15) shows that attitude errors are affected by gyro measurement errors $\boldsymbol{\delta\omega}_{ib}^b$ only. The equations (11, 13, and 15) form the INS error model to be used in Kalman filter in next section to predict errors in PVA for foot-mounted IMU. In state space format, the INS error model is represented as:

$$\begin{bmatrix} \boldsymbol{\delta}\dot{\mathbf{P}}^n \\ \boldsymbol{\delta}\dot{\mathbf{v}}^n \\ \boldsymbol{\delta}\dot{\boldsymbol{\psi}}^n \end{bmatrix} = \begin{bmatrix} \mathbf{0}_{3\times3} & \mathbf{I}_{3\times3} & \mathbf{0}_{3\times3} \\ \mathbf{0}_{3\times3} & \mathbf{0}_{3\times3} & -\mathbf{C}_b^n[\mathbf{f}^b\times] \\ \mathbf{0}_{3\times3} & \mathbf{0}_{3\times3} & \mathbf{0}_{3\times3} \end{bmatrix} \begin{bmatrix} \boldsymbol{\delta}\mathbf{P}^n \\ \boldsymbol{\delta}\mathbf{v}^n \\ \boldsymbol{\delta\psi}^n \end{bmatrix} + \begin{bmatrix} \mathbf{0}_{3\times3} & \mathbf{0}_{3\times3} \\ \mathbf{C}_b^n & \mathbf{0}_{3\times3} \\ \mathbf{0}_{3\times3} & -\mathbf{C}_b^n \end{bmatrix} \begin{bmatrix} \boldsymbol{\delta}\mathbf{f}^b \\ \boldsymbol{\delta\omega}_{ib}^b \end{bmatrix} \tag{16}$$

$$\delta\dot{\mathbf{X}} = \mathbf{A}\delta\mathbf{X} + \mathbf{B}\mathbf{W}$$

$$\therefore \delta\mathbf{X}^n \in \mathbb{R}^9; \boldsymbol{\delta}\mathbf{P}^n \in \mathbb{R}^3; \boldsymbol{\delta}\mathbf{v}^n \in \mathbb{R}^3; \boldsymbol{\delta\psi}^n \in \mathbb{R}^3; \mathbf{W} \in \mathbb{R}^6; \boldsymbol{\delta}\mathbf{f}^b \in \mathbb{R}^3; \boldsymbol{\delta\omega}_{ib}^b \in \mathbb{R}^3$$

The process noise, which consists of IMU zero-mean white noise sequences, has the covariance matrix **Q** defined by**:**

$$\mathbf{Q} = \mathrm{E}\{\mathbf{W}_n\mathbf{W}_n^T\} = \begin{bmatrix} \boldsymbol{\sigma}_{f^b}^2 & \mathbf{0}_{3\times3} \\ \mathbf{0}_{3\times3} & \boldsymbol{\sigma}_{\omega^b}^2 \end{bmatrix} \in \mathbb{R}^{6\times6} \tag{17}$$

where $\boldsymbol{\sigma}_{f^b}^2, \boldsymbol{\sigma}_{\omega^b}^2$ are variances of IMU. The discrete counter parts of matrices $\mathbf{A,B,Q}$ are obtained as follows:

$$\begin{aligned} \mathbf{F} &= \mathbf{I} + \mathbf{A}\Delta\mathbf{T} + \frac{1}{2}(\mathbf{A}\Delta\mathbf{T}) \\ \mathbf{G} &= \mathbf{B}\Delta\mathbf{T} \;\; ; \; \mathbf{Q}_d = \mathbf{BQB}^T \end{aligned} \tag{18}$$

If accelerometer and gyro bias vectors are also included in the state vector, then these terms are also augmented in state space model. However, as mentioned in [7], [8], these are not major error sources distorting the IMU output during high dynamic motions that the foot-mounted IMU is exposed to. Hence IMU bias error states are not included in EKF framework in this paper. However, Gyro bias should be estimated by averaging stationary data for few seconds initially before staring the experiment. The mean of the gyroscope readings for each axis must be subtracted from each subsequent measurement before utilizing them in PNS algorithm. This method works well even if the sensor is attached to a pedestrian's foot during calibration.

III. INS Adided with Virtual Sensors

As our aim is to use only single IMU as motion sensor and exploit the motion patterns of the walker to reduce drift in INS solution. Therefore, we will develop algorithmic virtual sensors which will constraint the INS errors as agent walks or remain stand-still during walking.

A. Zero-Velocity Update (ZUPT)

It is the natural process for human and legged animals as well, that when they walk in normal way, each time they push the ground backwards by their feet, at least one of the foot remains stationary for a while during ground contact. In other words, the velocity of that foot is momentarily becomes close to zero. If an IMU is mounted on that foot, it also experience brief cyclic stance phases during walk. If this zero-velocity moment is detected (algorithmically or by using contact sensors), this information may be fed to Kalman filter estimator to estimate the accumulated errors in PVA since last update of such knowledge. Since walking pattern repeats itself rapidly depending on the walking speed, i.e. stationary stance phase and moving stride phase, each lasts about 0.5~1 sec in normal walks. During stance phase, the zero-velocity updates are applied as 'pseudo-measurements' to the Extended Kalman filter, which utilize these measurements as correct knowledge and estimates the errors in PVA as its output.

1) Zero velocity detection algorithm: To detect the stance pases during walk, one can use actual contact sensors which sences the pressure exerted by foot on ground when it pushes the ground backwards during stance phase. However as the main idea of this paper is to use only single IMU sensor, so we will utilize IMU signlas only to detect the stationary periods.

For this, there are four commonly used methods or their combinations [8] in literature. These are: Acceleration Moving Variance Detector, Acceleration Magnitude Detector, Stance Hypothesis Optimal Detector (SHOE) and Angular Rate Energy Detector (ARE). However, it has been shown that ARE and SHOE are proved to be best in many experiments involving different gaits pattern [9]. Here we use ARE for stance detection in this paper. The brief description of ARE is as follows:

$$T(z_n^{\omega_{ib}^b}) = \frac{1}{W\sigma_{\omega_{ib}^b}^2}\sum_{k=n}^{n+W-1}\left\| y_k^{\omega_{ib}^b}\right\|^2; \qquad \therefore \left\| y_k^{\omega_{ib}^b}\right\|^2 = \sqrt{(\omega_{ib,x}^b)^2+(\omega_{ib,y}^b)^2+(\omega_{ib,z}^b)^2} \tag{19}$$

Where W is window size for weighted average of gyro signals ($y_k^{\omega_{ib}^b}$). T(.) is the test statics of the detector. Walking patterns are detected as:

$$Walk\ pattern(P_i) = \begin{cases} Stance\ phase: if\,(T(z_n^{\omega_{ib}^b}) < \gamma) \\ Stride\ phase: \text{otherwise} \end{cases} \tag{20}$$

The threshold (γ) is optimized based on experiments. This issue is not discussed in this paper.

2) Why Zero velocity update is important? The error growth in position is cubic with time while using only IMU, but this rapid growth can be circumvented by frequently aiding the IMU with ZUPT in EKF framework [10]. The ZUPT breakes this cubic growth by aiding after every 0.5 seconds or so and compensate for most of the errors of PVA and IMU, ie.g. position,velocity errors; accelerometer biases; pitch, roll errors, and the pitch and roll gyro biases. However the heading error and the heading gyro bias are the only important EKF states which are not observable from ZUPTs [11]. The unobservablity means the inability of EKF to estimate these states from a given sequence of measurements i.e ZUPTs. The relationship between velocity errors and attitude errors in n-frame is shown in (11), which can further be represented in component form for clarity [12]:

$$\begin{aligned} &\boldsymbol{\delta}\dot{\mathbf{v}}^n = \mathbf{C}_b^n[\mathbf{f}^b\times]\boldsymbol{\delta\psi}^n + \mathbf{C}_b^n\delta\mathbf{f}^b \\ &\therefore \boldsymbol{\delta}\dot{\mathbf{v}}^n = [\mathbf{f}^n\times]\boldsymbol{\delta\psi}^n + \delta\mathbf{f}^n \\ &\Rightarrow \begin{bmatrix}\boldsymbol{\delta}\dot{\mathbf{v}}^n\\ \boldsymbol{\delta}\dot{\mathbf{v}}^n\\ \boldsymbol{\delta}\dot{\mathbf{v}}^n\end{bmatrix} = \begin{bmatrix}0 & -f_D & f_E\\ f_D & 0 & -f_N\\ -f_E & f_N & 0\end{bmatrix}\begin{bmatrix}\delta\varphi\\ \delta\theta\\ \delta\psi\end{bmatrix} + \begin{bmatrix}\delta\mathbf{f}^n\\ \delta\mathbf{f}^n\\ \delta\mathbf{f}^n\end{bmatrix}\end{aligned} \tag{21}$$

Here $f_{N,E,D}$ is the acceleration in North, East, Down axis of the n-frame. Equation (21) shows that error in velocity is sum of error in acceleration measurement and error in attitude angles. In ZUPT algorithm, we use the velocity error as measurement in the stationary phase of the foot to correct PVA errors in EKF. During ZUPT, the horizontal forces in the local level frame are essentially zero ($i.e. f_N = f_N \approx 0$) and specific force f_D in downward direction is approximately equal to gravity constant. Therefore from equation (21), it is seen that the velocity errors in North and East directions are only related to errors in roll and pitch angles through a specific force f_D in downwards direction. Conceptually this means that during ZUPT period, the dynamic change in horizontal velocity is proportional to the change in roll and pitch errors. Improving the velocity estimation through ZUPT means that roll and pitch errors are improved as well but heading errors are not improved at all by ZUPT [11], [12]. Hence we have to use other methods to reduce drift in heading errors. For drift reduction in heading, we will use motion patterns such as, moving in staright paths, stading still for long time etc.

B. Walking Straight Paths:Straight trajectory heading (STH) Update

Human walks in straight paths, most of the times, in order to save time and energy. Also most of the corridors and hall ways are constructed straight in conventional buildings. When the user walks along these straight paths, this situation can be detected and exploited to reduce errors in gyro heading angle. A simple mechanism is used in this work to distinguish the near straight path from the curved path using average heading angle change during consecutive last n-footsteps in stance phase, i.e.

$$\Delta\psi_k = \psi_k - \frac{1}{n}\sum_{s=1}^{n}\psi_{k-s}$$

If $\Delta\psi_k > th.$, then we assume that user is walking in straight path and hence apply straight trajectory heading (STH) update.

C. Stading Still for long time:PA locking mechanism

Human are not always walking, but they have to stop at times during normal walking work. It has been observed that ZUPT does not guarantee complete stand-still condition [13]. Hence we have to devise another method to guarantee non-drift of PVA during complete stand still. We opted a simple method that tested experimentally and reduces error growth in position and attitude. When zero-velocity is detected, we check the forward velocity during this period, if it remains zero for extended period of time e.g. more than 5 seconds, it means that walker has stopped stepping forward and is in stand-still condition. If this condition is met, we apply simple rules to 'lock' the position and attitude at their current state, i.e.

$$\begin{aligned} &if\ v_x = 0\ \ for\ Time > thrs, \quad \therefore thrs = 5\sec. \\ &\quad \mathbf{P_k} = \mathbf{P_{k-1}} \quad \therefore \mathbf{P_k} \in \mathbb{R}^{3\times1} \\ &\quad \mathbf{q}_k = \frac{\mathbf{q}_{k-1}}{10^6} \quad \therefore \mathbf{q}_k \in \mathbb{R}^{4\times1} \\ &end \end{aligned} \tag{22}$$

i.e. position remains same and change in quaternion is negligible.

D. EKF algorithm for foot-mounted PNS

Final step is to fuse all valid motion information of the walker in an estimator in order to reduce error drifts in INS only solution. We have developed necessary models for EKF framework in previous sections, and now present formally the prediction and update part of the estimator as shown in Fig. 2. In discrete time domain, the EKF prediction and update cycles are summarized here:

i) Initialize the filter as follows:

$$\delta\hat{\mathbf{x}}_0^+ = \mathbf{E}(\delta\mathbf{x}_0) \tag{23}$$

$$\mathbf{P}_0^+ = \mathbf{E}[(\delta\mathbf{x}_0 - \delta\hat{\mathbf{x}}_0^+)(\delta\mathbf{x}_0 - \delta\hat{\mathbf{x}}_0^+)^T]$$

For *k=1, 2,...., N*, perform the following:

ii) Obtain discrete state transition matrices:

$$\mathbf{F} = \mathbf{I} + \mathbf{A}\Delta\mathbf{T} + \frac{1}{2}(\mathbf{A}\Delta\mathbf{T})^2 \tag{24}$$

$$\mathbf{G} = \mathbf{B}\Delta\mathbf{T};\ \mathbf{Q} = \mathbf{B}\mathbf{Q}_c\mathbf{B}^T$$

iii) Perform the propagation step:

$$\delta\hat{\mathbf{x}}_k^- = 0 \tag{25}$$

$$\mathbf{P}_k^- = \mathbf{F}_{k-1}\mathbf{P}_{k-1}^+\mathbf{F}_{k-1}^T + \mathbf{G}_{k-1}\mathbf{Q}_{k-1}\mathbf{G}_{k-1}^T$$

iv) Perform the measurement update step:

$$\mathbf{k}_k = \mathbf{P}_k^-\mathbf{H}_k^T(\mathbf{H}_k\mathbf{P}_k^-\mathbf{H}_k^T + \mathbf{R}_k)^{-1} \tag{26-1}$$

$$\delta\hat{\mathbf{x}}_k^+ = \delta\hat{\mathbf{x}}_k^- + \mathbf{k}_k[\mathbf{z}_k^n - \mathbf{h}(\delta\hat{\mathbf{x}}_k^-, 0)] \equiv \mathbf{k}_k[\delta\mathbf{z}_k^n] \tag{26-2}$$

$$\mathbf{P}_k^+ = (\mathbf{I} - \mathbf{k}_k\mathbf{H}_k)\mathbf{P}_k^- \tag{26-3}$$

v) Feedback correction of PVA:

$$\begin{aligned} {}^c\mathbf{P}_k^n &= \mathbf{P}_k^n - \delta\hat{\mathbf{x}}_{k,\mathbf{P}}^+ \\ {}^c\mathbf{v}_k^n &= \mathbf{v}_k^n - \delta\hat{\mathbf{x}}_{k,\mathbf{V}}^+ \\ {}^c\mathbf{C}_{b,k}^n &= (\mathbf{I} - [\delta\hat{\mathbf{x}}_{k,\psi}^+ \times])^{-1}\mathbf{C}_{b,k}^n \end{aligned} \tag{27}$$

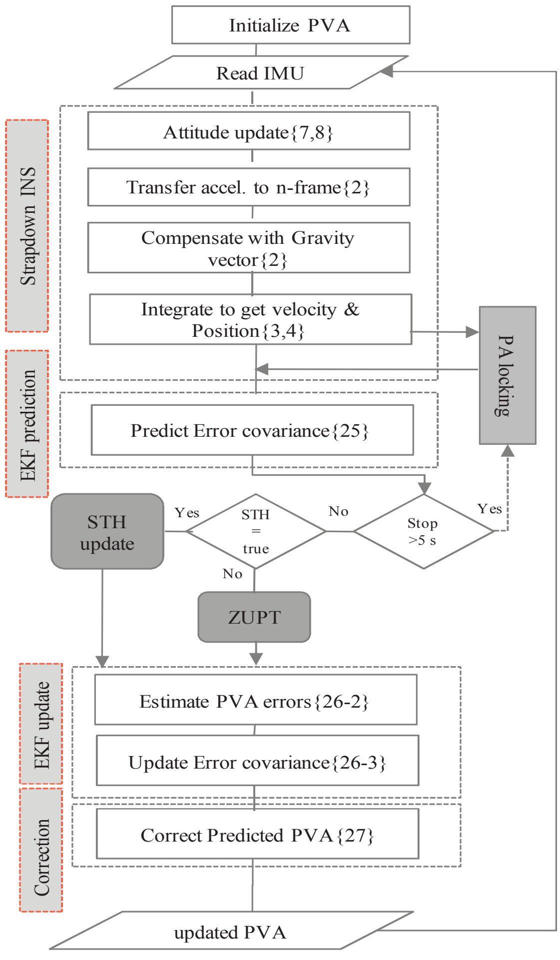

Fig. 2. EKF algorithm flowchart: Data fusion of INS, ZUPT, STH,PA-locking

IV. Experiments and Results Discussion

To verify our proposed methods, we conducted experiments in both outdoor and indoor environment, with no prior information about the test environment. The IMU (3DM-GX3-25) from Microstrain Inc. is used for data collection.

Although this IMU provides many kinds of navigation data, but we picked up only raw accelerometer and gyro data and rest of the navigation solution and data processing is done in our own designed algorithm. The IMU was fitted on the left foot and the walker walked with normal way. In outdoor experiment, we also deliberately changed walking direction randomly(Fig. 3), e.g. in segment A, walking is back-footed; in segment B, walking is side-steps, and similarly in segment C, walker walked with side-steps, changing directions 180 degree randomly, in order to check the robustness of the designed algorithm.

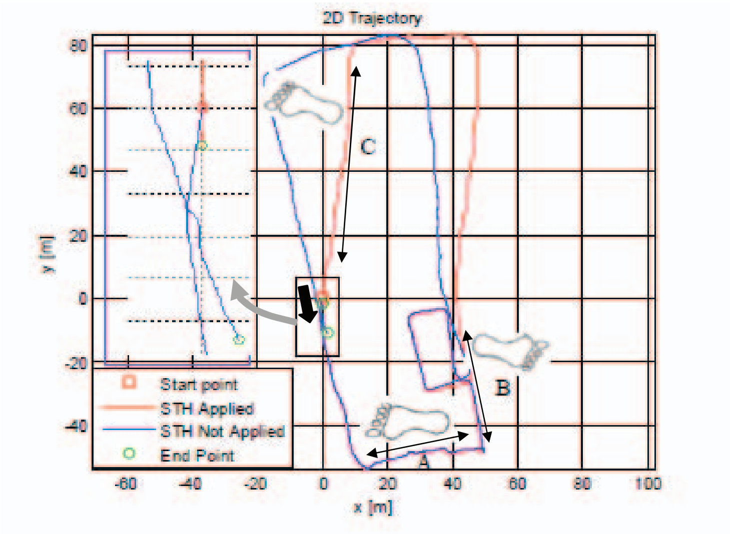

Fig. 3. 2D trajectory plot comparison in outdoor test. Top left window is zoomed view of the end points.

In Fig. 3, we show the results of applying the STH algorithm as aiding virtual sensor to INS. The Fig. 4 shows the real trajectory (about 450m) for visual inspection. It is clear that when we apply STH conditions, the trajectory estimated with INS/ZUPT/STH algorithm is more like to the real one as compared to the trajectory when no STH applied. For quantitative comparison, we checked the end trajectory errors (RMSE) and shown in Table I.

Fig. 4. Actual 2D trajectory drawn manually on Google maps for visualization of actual path traveled.

Similar analysis is done in indoor tests as well, as shown in Fig. 5 and 6. The indoor test was conducted in a three storey building in KITECH, with double flight stairs to change floor. In Fig. 5 and 6, the red trajectory keeps the parallelism and perpendicularity of the building layout, but blue trajectory is not aligned with building layout. It shows the effectiveness of simple STH method applied. The reason is that most buildings have straight corridors and hence STH is more effective in indoor environment.

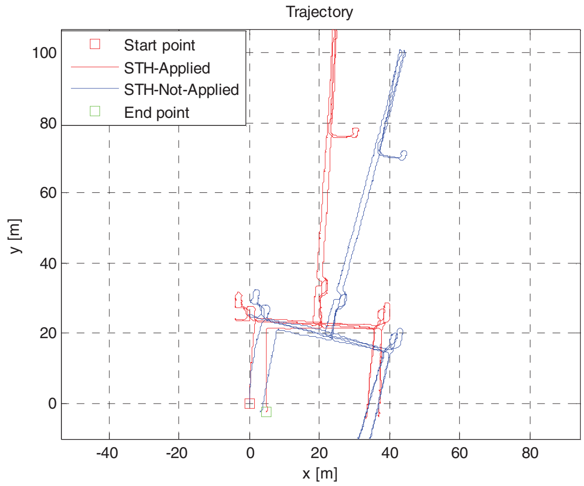

Fig. 5. 2D trajectory plot comparison in indoor test. Effect of STH applied.

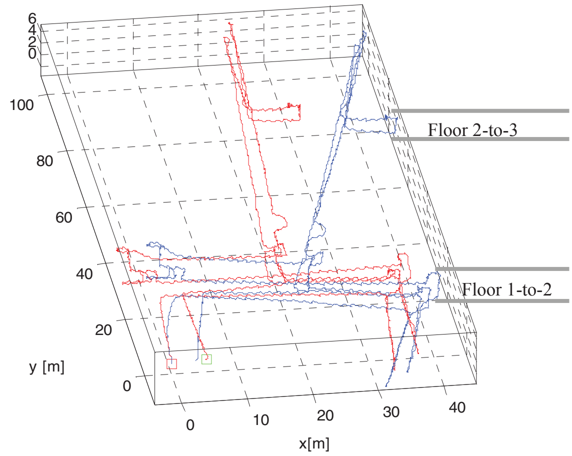

Fig. 6. 3D trajectory plot of indoor testing (3-storey building in KITECH). Effect of STH applied.

To check the second algorithm, i.e. position and attitude locking when the user is found standing still for long time (e.g. >5sec.), we did walking experiment with frequent stop-and-go fashion. The results are shown in Fig. 7. It is seen that with PA-locking applied, the error in final reach point and errors in attitude angles are reduced, as shown in Fig. 8. The RMSE results are tabulated in Table II.

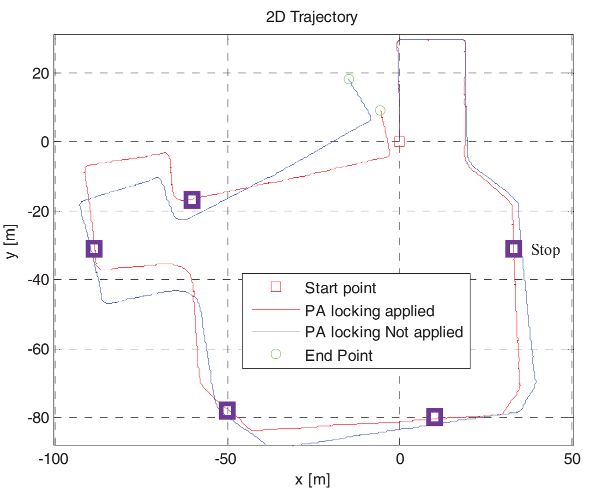

Fig. 7. Outdoor trajectory with frequent stop-and-go walk to check the effectiveness of PA locking mechanism on position drift.

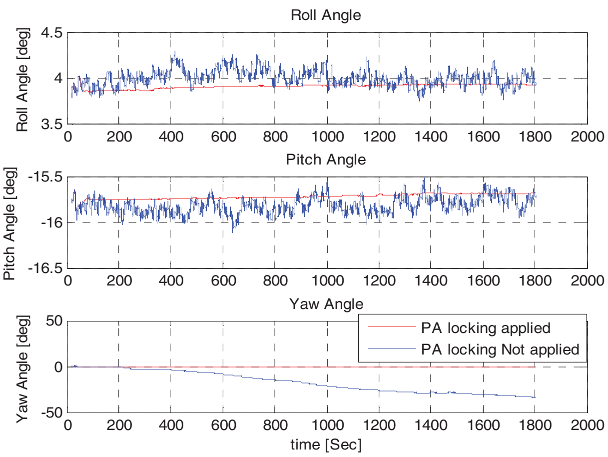

Fig.8. Static data for 30 minutes to check the effects of PA locking mechanism on attitude.

TABLE I. RMSE ERROR IN INDOOR/OUTDOOR MOVING TEST

Test	**Description**	**Dist(m)**	**Time (min)**	**Return Position Error(m)**			
				STH aided		***No STH aided***	
				2D Error	***3D Error***	***2D Error***	***3D Error***
Out door	Closed double loop	450	10	1.7	2.5	11	11.14
In door	Multi floor	360	15	2.1	2.5	4.6	5.1

TABLE II. RMSE ERROR IN STATIC AND STOP-AND-GO TEST

Test Description	**Dist(m)**	**Time (min)**	**Return Position Error(m)**			
			PA Locking applied		***PA Locking not applied***	
			2D Error	***3D Error***	***2D Error***	***3D Error***
Static	----	30	0.1	0.2	2.2	3.5
Moving	430	17	10.6	11.2	23.3	23.5

V. CONCLUSION AND FUTURE WORK

We presented pedestrian navigation system using foot-mounted IMU and exploiting motion patterns of the walker, with no prior information about the test environment and the user itself. It is found that it is very cheap, simple and infrastructure-free solution for PNS applications to use the single MEMS IMU and motion knowledge of the walker and estimate the errors in INS. After conducting experiments in indoor and outdoor environment, we conclude that errors in IMU-only navigation solution are reduced drastically by analyzing only the motion constraints and without using any other external sensors or knowledge about the walker or test environment. As a future research, we aim to investigate the fusion of IMU data fitted on foot and aid INS with height sensor (barometer) and magnetometer, which are part of most the MEMS IMUs today. Additionally, to solve the inherent heading drift problem in INS, we intend to add small 2D lidar on appropriate body part.

REFERENCES

[1] R. Feliz, E. Zalama and J. G'Omez, "Pedestrian tracking using inertial sensors," Journal of Physical Agents, vol 3, no.1, pp.35-42, 2009.

[2] A. R. Jim´enez, F. Seco, J.C. Prieto and J. Guevara, "Indoor pedestrian naigation using an INS/EKF framework for yaw drift reduction and a foot-mounted IMU," in Proceedings of 7th Workshop on Positioning, Navigation and Communication, WPNC 2010, Dresden, Germany, March 11-12, 2010.

[3] P. D. Groves , Principles of GNSS, Inertial, and Multisensor Integrated Navigation Systems, Artech House, 2008.

[4] D. H. Titterton, J. L. Weston, Strapdown Inertial Navigation Technology, 2nd edition, Institute of Engineering and Technology, UK, 2004.

[5] J. L. Farrell, GNSS Aided navigation and Tracking-Inertially Augmented or Autonomous, Amercan Literary Pres, 2007.

[6] J. Kim "Autonomous navigation for airborne applications," PhD dissertation , ACFR, The University of Sydney, May 2004.

[7] I. Skog and J-O Nilson, "Evaluation of zero-velocity detectors for foot-mounted inertial navigation systems," in International Conference on Indoor Positioning and Indoor Navigation (IPIN), Zurich, Switzerland, 15-17 September 2010.

[8] I. Skog, P. Handel, J-O Nilson and J. Ranatakokko, "Zero-velocity detection-an algorithm evaluation," IEEE Transactions on Biomedical Engineering, vol. 57, no. 11, pp. 2657-2665, 2010.

[9] J-O Nilson, I. Skog and P. Handel, "A note on the limitations of ZUPTs and the implications on sensor error modeling," in International Conference on Indoor Positioning and Indoor Navigation (IPIN), November 2012.

[10] E. Foxlin, "Pedestrian tracking with shoe-mounted Inertial sensors," Moving Mixed reality into the real word, IEEE Computer society, December 2005.

[11] K. Abdulrahim, C. Hide, T. Moore and C. Hill , "Aiding low cost inertial navigation with building heading for Pedestrian navigation," The Journal of Navigation, vol.64 , pp. 219–233, 2011.

[12] S. He, "Integration of multiple sensors for astronaut navigation on the lunar surface," PhD dissertation, Ohio State University, 2012.

[13] J-O Nilson and P. Handel, "Standing still with inertial navigation," in International Conference on Indoor Positioning and Indoor Navigation (IPIN), October 2013.